

Article

One step mechanosynthesis of graphene oxide directly from graphite

Victor Gerardo Ibarra-García¹, Demetrio Mendoza-Anaya², Alma Victoria Sánchez-Mendoza¹, Rosa Angeles Vázquez-García¹, Karina Alemán-Ayala¹, Màrius Ramírez-Cardona¹, and Victor M. Castaño^{3,*}

¹ Área Académica de Ciencias de la Tierra y Materiales, Área Académica de Computación y Electrónica, Universidad Autónoma del Estado de Hidalgo, Cd. Universitaria, C.P. 42184 Pachuca, Hgo., México.; vicgig90@outlook.com

² Instituto Nacional de Investigaciones Nucleares, Carretera México - Toluca S/N, La Marqueza.

³ Centro de Física Aplicada y Tecnología Avanzada (CFATA), Universidad Nacional Autónoma de México, Boulevard Juriquilla 3001, Querétaro 76230, México; vmcastano@unam.mx

* Correspondence: vmcastano@unam.mx; Tel.: +52-1442-156-0915 (V.M.C)

Abstract: Graphene oxide was synthesized by a one-step environmentally friendly mechanochemistry process directly from graphite and characterized by Raman, FT-IR and UV/vis spectroscopies, Atomic Force Microscopy, X-ray Diffraction, Scanning Electron Microscopy, Energy-Dispersive X-ray Spectroscopy and Thermogravimetric Analysis. Spectroscopic analysis shows that the functional groups and oxygen content of the synthesized material are comparable with those of graphene oxide synthesized by other previously reported methods (Hummers). Thermogravimetric analysis reveals thermal stability up to 400 °C.

Keywords: Graphene; graphene oxide; mechanochemistry; solvent-free; one-step.

1. Introduction

The work of Novoselov and Geim [1] caused an exponential growth in research on graphenic materials. Although graphene is a single layer of sp² carbon atoms of just 1 atom thickness, other graphenic materials exist, such as bi-layer, few-layered (1-3 layers), multi-layered graphene sheets (4-10 layers) [2], thick-layer graphene (>10 layers) [3], graphene ribbons [4], or Chemically-Modified Graphenic materials (CMG). The latter have received great deal of attention in recent years because the chemical methods followed for their production may be scaled up to high rates of production [5,6] and also serve as precursors of graphene.

CMG is a group composed by graphene oxide (GO) and reduced graphene oxide (rGO). Both of them are graphene-containing hydroxy, epoxy, keto and carboxylic acid groups, however, the latter is, as its name implies, GO that has undergone a reduction process, thus decreasing the amount of carboxylic and keto groups. Regularly, this involves the submersion of GO in hydrazine, although some greener methods have been developed [7, 8].

CMG have been successfully employed as humidity sensors [9], biosensors [10-12], photothermal agents in treatments against cancer [13] or Alzheimer's disease [14], antibacterial agents [15], battery electrodes [16] and power generation devices [17].

Although GO has been known for more than fifty years [18] it was dubbed graphite oxide. And until recently, most works about the production of GO are based on that of Hummers and Offeman (Hummers' method or graphite oxide route). Nevertheless, recently, new methodologies are starting to be developed for the synthesis of CMG. For instance, electrochemistry [19,21] and sonochemistry [5]. Although they reduce the time required for the synthesis of CMG, they still require acids for their synthesis and relatively high temperatures [5].

Mechanochemistry (MC) can be formally described as the discipline that deals with chemical reactions induced by mechanical input. Although regularly regarded as a solid-state only approach, several works show the feasibility of mechanosynthesis in every aggregate state [22-24]. Recent works

show how this kind of chemistry offers many advantages over traditional chemistry, being the most important one the decrease on reaction time and use of catalyzers.

For instance, via MC the degradation of ibuprofen can be achieved after only 40 hours [25,26] vs. up to 8 months using traditional methods [27], the production of cellulosic fibers can be carried on in just 1 hour [28] and the production of organic compounds like biaryls and aldehydes is carried on in just a couple of minutes with yields of more than 91% [29], all these while also greatly decreasing the use of solvents [29,30].

Research about mechanochemistry on carbonaceous materials such as graphenic materials, fullerenes, quantum dots [31] or carbon nanotubes [32] is an active field. Until now, several processes for the modification of graphenic materials via MC have been developed. Most of them modify already existent CMG, such as the reduction of GO using under inert atmosphere [33] or the production of graphene oxide platelets from GO [34].

However, only a few functionalize graphene. Examples of this are the selective edge functionalization of graphene using graphite and dry ice as precursors, which takes place in 48 h. [35], the edge carboxylation of graphene in presence of dry ice, hydrogen and sulphur trioxide, which also occurs in 48 h [36], the synthesis of GO via MC using KMnO_4 and aspartic acid in 24 h [37], and the production of hydroxyl-graphene from graphite and KOH after 8 hours of mechanical milling using a planetary ball mill [38]. These works show that GO synthesis can be carried out using mechanical milling. All these works use catalyzers for the transformation.

To the extent of our knowledge, there is just one process reported on literature in which the use of graphite alone is reported to produce GO [39]. In that work, a planetary ball mill is used to synthesize GO after 8 hours. Nevertheless, in our group we discovered that the synthesis of GO can be carried out in less than 4 hours from graphite alone as reagent via a mechanochemistry process using a SPEX 8000D mixer mill.

2. Materials and Methods

2.1 Mechanochemistry of graphene oxide

Mechanochemistry (MS) was carried out in a SpeX 8000D mixer mill, using a steel vial (capacity of 10g) with six hardened steel milling balls (8.3g weight each). 1g of expandable graphite obtained from Sigma-Aldrich was introduced in the vial and milled for up to 4 hours at 1725 rpm. After the processes finished, the resulting material was extracted and characterized. Samples were ultrasonicated for 2 hours using EtOH, and then, they were washed with absolute grade ethanol and filtered using 0.45 μm PTFE membranes from GE Healthcare. Next, they were dried for their characterization. All the reagents were purchased by Aldrich and used as received. The solvents were from J.T. Baker.

2.2 Instruments

Infrared (IR) spectra were acquired on a FT-IR Perkin Elmer model Frontier instrument, using pellets of KBr. The UV-Vis absorption spectra were obtained in a Perkin Elmer XLS equipment, using EtOH as solvent. Raman spectra were obtained in a Bruker, model Senterra apparatus, with a resolution of 9-15 cm^{-1} , after 6 scans and 8 seconds of integration.

Microstructural characterization was performed in a JEOL JSM-5900LV scanning electron microscope (SEM), with coupled energy X-ray dispersion spectroscopy (EDS). The images were taken with a secondary electron signals at 30 kV, in the high vacuum mode. To identify the crystalline phases in the samples, the X-ray diffraction (XRD) technique was conducted using a D8 Discover Bruker diffractometer with monochromatic $\text{Cu-K}\alpha$ radiation ($\lambda=1.5418 \text{ \AA}$). The XRD patterns were obtained, in the range from 10 to 60 in 2-theta degree, with a step size of 0.03°, at 40 kV and 40 mA; measurements were performed directly on the powder samples.

The morphological characterization by AFM was carried out using an Asylum Research scan probe microscope model Cypher; samples were prepared by depositing dispersions of graphene oxide in ethanol on a freshly cleaved mica surface (Ted Pella, Inc.) and allowing them to drying air.

Thermogravimetric analysis was done using a Mettler-TOLEDO Model 851e instrument. Ultrasonication of the samples was done using an AS20500 AT ultrasonic cleaner from Autoscience.

3. Results and Discussion

The synthesis of the graphene oxide was carried out by means of a mechanochemistry method. The formation of graphene oxide with different functional groups was observed after 30, 60, 120 and 240 minutes of milling without use of inert atmosphere or added catalysts or solvents.

UV spectra for samples corresponding to 0.5 y 4 hours of mechanochemistry (MS) are shown in figure 1. In both of them, four features can be observed: three bands, one at 214 nm, a second one at 219 nm, a third one at 222 nm, and lastly, a shoulder at 288 nm for the spectrum of samples synthesized after 0.5 hours of MS; and one at 220 nm, a second one at 223 nm, a third one at 234 nm and a fourth one at 280 nm for the spectrum from samples synthesized after 4 hours of MS. According to previous reports [3,33,40], the bands from 214 nm to 223 nm of either spectrum are produced by the π - π^* transitions of aromatic C=C rings. The features at 280 and 288 nm of both spectra are due to the π - π^* and n- π^* transition of C-O groups.

The bands related to the π - π^* transitions of the C=C matrix correspond with what has been reported in the aforementioned works and indicate that the sp² carbon matrix has been disrupted in different ways between samples of 0.5 hours and 4 hours of MS.

In our spectra the features of 280 and 288 nm show an important difference. For samples from 0.5 hours of MS the feature is a shoulder, this suggests the presence of C-O groups, although their abundance is low. In contrast, the feature of samples from 4 hours of MS is a band, which suggests a higher abundance of C-O groups than in samples from 0.5 hours of MS.

This is supported by previous reports [3,40] where it is demonstrated that the intensity of the band at around 320 nm depends on the degree of oxidation of the samples and also with the report of Luo, *et al.* [40], where that signal becomes fainter as GO undergoes a reduction process.

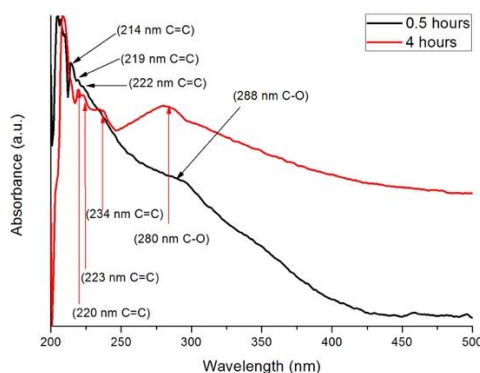


Figure 1. UV-vis spectra of GO synthesized at 4 hours

In figure 2 which shows the FT-IR spectra from samples obtained after 0.5 and 4 hours of MS, the characteristic bands of graphene oxide appear [33,41,42]. The band at 3426 cm⁻¹ corresponding the longitudinal stretching vibration of hydroxyl groups (O-H) [43], the longitudinal vibration of the C=C segments from graphenic sp² matrix at 1586 cm⁻¹ [41,44], the bands of C=O at 1631 cm⁻¹ in both samples [45] and at 1723 cm⁻¹ and 1746 cm⁻¹ for samples synthesized after 0.5 and 4 hours of MS respectively [43, 41]. The band at 1429 cm⁻¹ (δ , C-OH) indicates the presence of carboxylic acids (COOH) according to [41,45,46,47].

In addition to these bands, two more appear at 2920 cm⁻¹ and 2850 cm⁻¹, these correspond to -CH groups [42], this indicates the presence of epoxide groups, which is corroborated with the band at 1098 cm⁻¹. Also, this -CH groups may be the cause of the blue shifted bands observed in UV spectroscopy. This because the sp³ carbons decrease the conjugation of the sp² carbon matrix. Only

few works that involve graphene oxide synthesized by methods not related directly to the Hummers method report these bands.

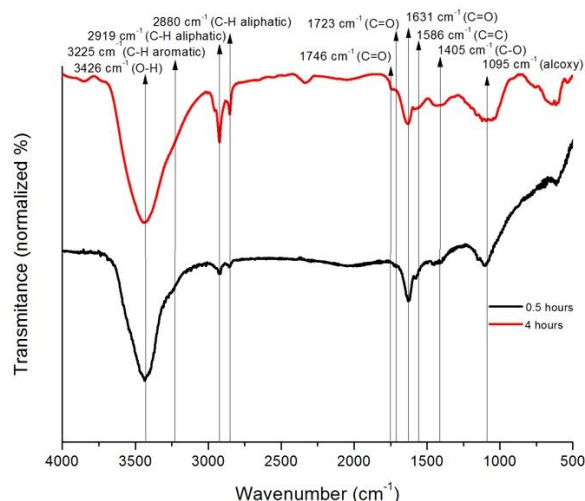


Figure 2. FT-IR spectra from samples synthesized after 0.5 and 4 hours of MS.

Further on, Raman characterization was carried out. The spectrum corresponding to samples synthesized after 4 hours of MS is shown in Figure 3. It shows the characteristic features of graphene oxide [48-51]. The first one, the band at 1403 cm^{-1} (D band), the second one, the band at 1684 cm^{-1} (G band) and that at 1698 cm^{-1} (D' band). The first one is caused by the edges of the graphenic lattice, which increase due to the reduction of the lateral size of the sheets, the disruptions in the sp^2 matrix caused by the oxygenated groups [49,52,53] and lattice holes, which presence are confirmed by FT-IR spectroscopy; the second one by the in-phase vibration of the graphenic lattice [49,52], which is inherent to graphenic materials; and the third one, which being related to defects in the sp^2 matrix due to phonon confinement, suggests that there are numerous structural defects in the samples, this agrees with another work where mechanical milling is evaluated [54]. When analyzing the intensity of the signals, the I_D/I_G ratio is 1.88 which is higher than the reports from other authors [42, 52, 55, 56]. This indicates that the graphenic sp^2 carbon lattice has been disrupted in an important way, either by the addition of oxidized groups or the breakage of the graphenic layers, which is inherent to the synthesis process.

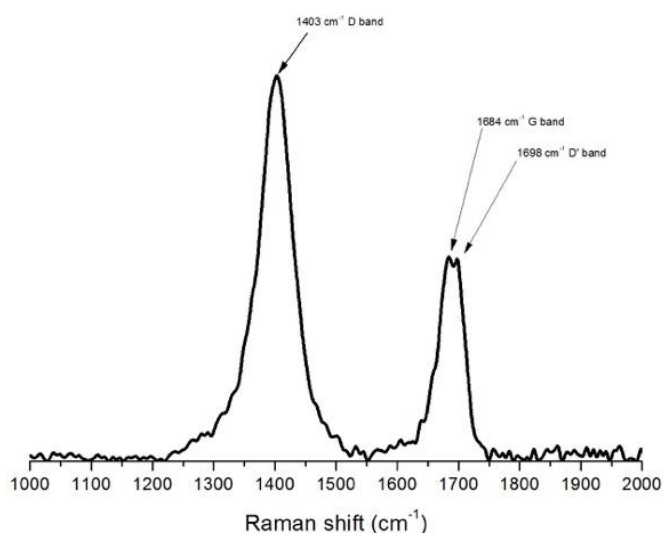


Figure 3. Raman spectra from samples synthesized after 4 hours of mechanical milling.

Figure 4 shows two SEM micrographs at different magnifications (10k and 20k). These micrographs revealed that the material consists of randomly aggregated, thin, crumpled sheets

closely associated with each other and forming a disordered solid. Figure 5 shows 2 SEM micrographs at 20k, in which the lamellar structure is appraised.

Elemental chemical analysis using the EDS technique is shown in Table 1. It is possible to observe that carbon and oxygen are the main elements present in the sample with a low amount of sulphur (which is due to the raw material). It is worth mentioning that for these samples, the average oxygen content is 13 wt%, while other authors report greater amount of it (≈ 30.37 w%), however, they used the XPS as detection technique [57].

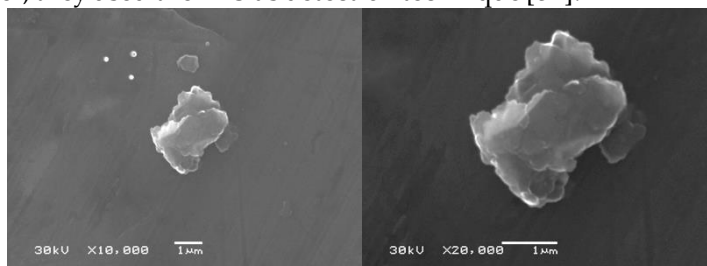


Figure 4. SEM microphotographs from sample synthesized after 4 hours of MS at x10k and x20 k .

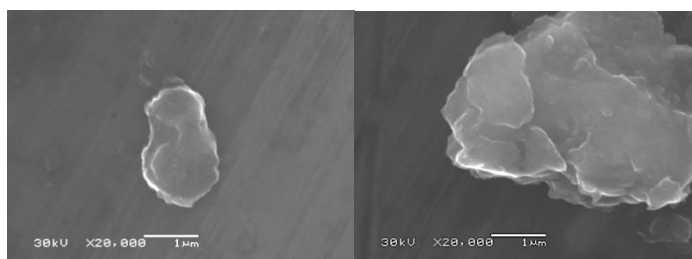


Figure 5. SEM microphotographs from sample synthesized after 4 hours of MS at x20k

Table 1. Elemental compositions obtained with EDS from samples synthesized after 4 hours of mechanical milling.

Element	Figure 4 (right)		Figure 5 (right)	
	wt%	at.%	wt%	at.%
C	83.55	87.95	85.13	89.41
O	14.07	11.11	12	9.46
S	2.38	0.94	2.87	1.13

Figure 6 shows an atomic force microscopy (AFM) image of the material synthesized after 2 hours of mechanical milling; it corresponds to a typical graphene oxide AFM image. A layered structure is observed, which confirms the features resembling a layered structure observed during SEM studies. This result is in agreement with the expected graphene oxide structure. The material could be classified as a multilayer graphene oxide, nevertheless, for AFM studies the sample was sonicated for less than 5 minutes so the material was not completely exfoliated, thus it could still reduce its thickness if it undergoes sonication for a longer period of time.

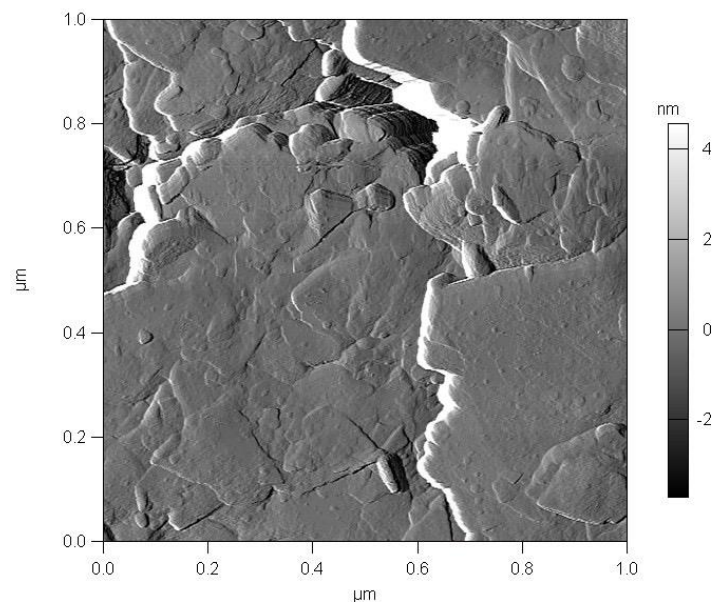


Figure 6. AFM image of material synthesized after 2 hours of mechanical input.

The TGA curve of graphene oxide synthesized after 2 h of MS is shown in figure 7. It is possible to observe an important weight loss starting at 423.167 °C, which is higher than the reported results by other groups. We suppose, it is related to presence of less thermolabile groups, such as keto and epoxy groups, which are shown in FT-IR studies.

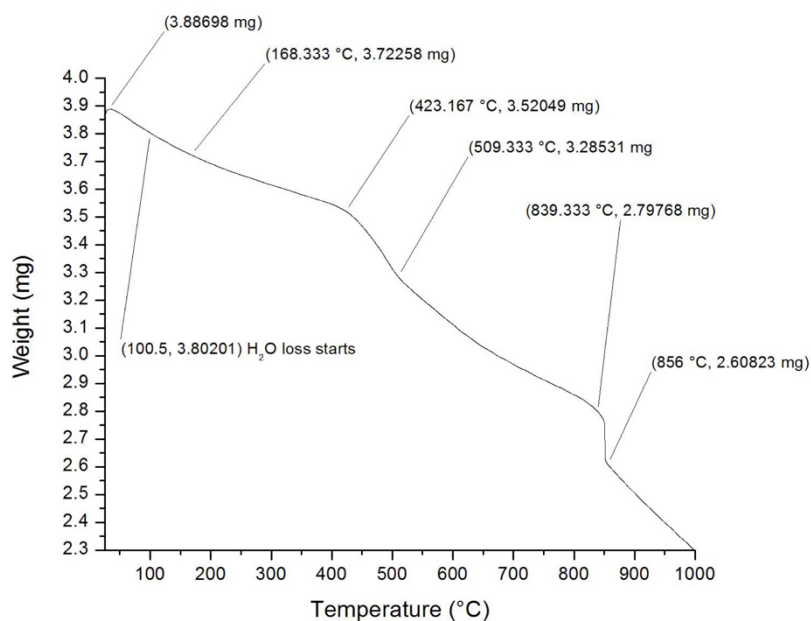


Figure 7. TGA plot from sample obtained after 2 hours of MS.

Finally, XRD analysis was used to characterize the crystalline nature and phase purity of the as-synthesized GO and graphite. With this technique it can be confirmed the presence of graphite and graphene oxide in the studied samples, as can be observed in figure 8. The former is confirmed by the two diffraction peaks at 26.34° and 54.91° 2- theta. The latter because after sonication two phases formed; one that precipitated in the bottom of the flasks and the other that was suspended in the solvent (ethanol). When analyzing both of them separately a wide diffraction peak at 13.49° 2- theta can be observed, which is assigned to the (001) plane of graphene oxide. For the soluble phase the signal is more intense than the signal from graphite, in contrast, the intensity of the signal from the insoluble phase is roughly 25% of the signal from graphite. This indicates that the species that

generates the signal has a hydrophilic character. This is in line with what FT-IR spectra showed. Also, this confirms that the D band in the Raman spectrum is due to the incorporation of oxygenated groups and not just the appearance of defects, such as holes in the C=C matrix, or the reduction of the lateral size of graphenic sheets due to mechanical milling.

It is important to mention that the assigned peak to graphene oxide in this work (13.49°) is among the reported values in other works, such as, 11.3° [58], 8° - 9.5° [53], 10.27° [59], 15° [60] and 14.45° [61]. Numerous works show that the interlayer spacing is given on function of the oxidation degree of the sheets [53] and the interaction between solvent and graphene oxide [62]. The higher the oxidation degree and solvent abundance, the higher the interlayer space is and vice versa. Although there is not a consensus about how thick a graphene oxide sheet is or how big the d-space must be, some authors like Zheng *et al.* report a 0.8 nm thickness for dry GO [65], and past reports do state that d-space can grow from 0.57 nm to 0.79 nm when passing from 0 % to 25 % of relative humidity [60]. One of the advantages of MS on conventional synthesis is that it avoids the use of solvents, and our process is carried on without the need of adding water or solvents; therefore, when contrasting the XRD and EDS results, we assume that although the degree of oxidation from our samples is lower to those reported by other authors, it allows a d-space “high” enough to exfoliate sheets and that this d-space is low because of the lack of solvent in the material. The latter because even when sonicated for 2 hours in presence of ethanol, and after separating both phases they were left to dry at atmospheric conditions, Sheng *et al.* [65] state that 120 hours were needed to completely soak GO and ethanol was found to be less wetting on GO than water.

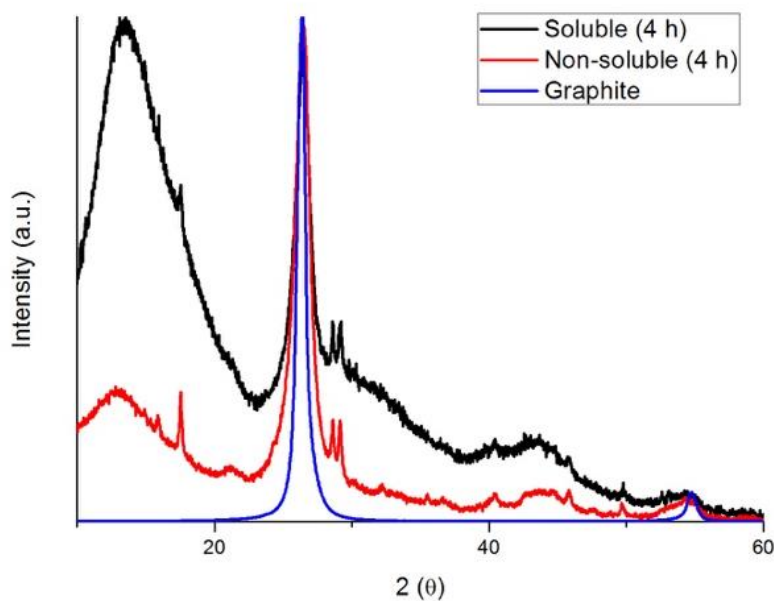


Figure 8. XRD analysis of graphite and synthesized GO.

Along with the aforementioned, signals we also observe a number of signals with high intensities. At 15.96° , 17.5° , 21.13° , 29.17° , 28.67° in 2-theta. We discard them being due to contamination from the degradation of the steel vial based on the EDS studies were less than 2 at.% of other elements apart of C and O were detected. Some of them may be generated by a new crystalline phase, nevertheless more studies are needed to confirm that, yet the signal at 15.96° and 17.52° in 2-theta could be due to GO but with a lower interlayer space.

Considering all evidence presented above, the interlayer spacing and the amount of solvent present in our material must be the causes for its higher thermal stability. This because there is evidence that the interaction between solvent molecules and the graphenic layers dictate the transformations that the material undergoes in function of its temperature [64]. The aforementioned evidence shows that the interlayer spacing in our material is lower than that reported before by several authors. This should decrease the mobility of solvent between layers. Considering that the

amount of solvent present in our material is low, and that the number of defects in the graphenic layers that comprise it is relatively high, we assume that the dynamics of chemical transformation undergone by the material when increasing its temperature are different from that produced by methods related to that of Hummers.

This because the number of “edges” increases when holes are created within the layers and, although graphene oxide is not a stoichiometric compound, the transformation of oxidized groups differ when occurring near the edges and within the sheets. And being the rate of these transformations in function of the available solvent, which in our material is low because of the reasons stated lines above, we conclude that in the present material these situations happen and transformations become more difficult to occur, thus altering the thermal stability of the material, in this case, increasing it.

5. Conclusions

The results demonstrate that mechanosynthesis is an eco-friendly and affordable method that allows the synthesis of graphene oxide directly from graphite. We have demonstrated that with this chemical approach we can produce oxidized graphene in 4 hours, without adding any solvent, acid or oxidizing agent. Also, that the material produced this way is equivalent to GO synthesized via the Hummers method. Lastly, a new crystalline phase of graphite could have been synthesized as a co-product.

6. Patents

The patent application MX/a/2018/015685 has been submitted to the Instituto Mexicano de la Propiedad Industrial to protect the results shown on this article.

Author Contributions: Conceptualization, V.G.I-G., R.A.V-G. and V.M.C.; methodology, V.G.I-G., R.A.V-G. and V.M.C.; validation, all authors; investigation, V.G.I-G, A.V.S-M and D.M-A.; resources, K. A-A. and V.M.C.; writing—original draft preparation, all authors.; writing—review and editing, all authors; visualization, all authors; supervision, R.A.V-G., V.M.C. and D.M-A.; project administration, R.A.V-G. and V.M.C.; funding acquisition, V.M.C.

Funding: SDI-UNAM-2019.

Acknowledgments: The authors are indebted to Dr. Genoveva Hernández-Padron for her assistance with Raman analysis, Dr. Heberto Gómez Pozos for his support for the development of this work and Dr. Fidel Perez Moreno for his support with TGA analysis. Victor Gerardo Ibarra-García thanks Consejo Nacional de Ciencia y Tecnología (CONACYT) for the scholarship received during his PhD studies (Scholarship number: 429038)

Conflicts of Interest: “The authors declare no conflict of interest.”

References

1. Novoselov, K. S., Geim, A. K., Morozov, S. V., Jiang, D., Zhang, Y., Dubonos, S. V., . . . Firsov, A. A. (2004). Electric Field Effect in Atomically Thin Carbon Films. *Science*, 306(5696), 666-669. doi:10.1126/science.1102896
2. Martín, A., & Escarpa, A. (2014). Review: Graphene: The cutting-edge interaction between chemistry and electrochemistry. *Trends in analytical chemistry*, 13-26.
3. Lai, Q., Zhu, S., Luo, X., Zou, M., & Huang, S. (2012). Ultraviolet-visible spectroscopy of graphene oxides. *AIP Advances*, 2(3), 2–7. <https://doi.org/10.1063/1.4747817>
4. Wu, Z.-S., Ren, W., Gao, L., Liu, B., Zhao, J., & Cheng, H.-M. (2010). Efficient Synthesis of Graphene Nanoribbons Sonochemically Cut from Graphene Sheets. *Nano Research*, 16-22.
5. Yang, H., Li, H., Zhai, J., Sun, L., & Yu, H. (2014). Simple Synthesis of Graphene Oxide Using Ultrasonic Cleaner from Expanded Graphite.

6. Zhang, L., Liang, J., Huang, Y., Ma, Y., Wang, Y., & Chen, Y. (2009). Size-controlled synthesis of graphene oxide sheets on a large scale using chemical exfoliation. *Carbon*, 47(14), 3365–3368. <https://doi.org/10.1016/j.carbon.2009.07.045>
7. Zhu, C., Guo, S., Fang, Y., & Dong, S. (2010). Reducing sugar: New functional molecules for the green synthesis of graphene nanosheets. *ACSNANO*, 2429-2437
8. Zhang, J., Yang, H., Shen, G., Cheng, P., Zhang, J., & Guo, S. (2010). Reduction of graphene oxide via L-ascorbic acid. *Chemical Communication*, 46(7), 1112–4. <https://doi.org/10.1039/b917705a>
9. Borini, S., White, R., Wei, D., Astley, M., Haque, S., Spigone, E., . . . Ryhänen, T. (2013). Ultrafast Graphene Oxide Humidity Sensors. *ACS Nano*, 7(12), 11166-11173. doi:10.1021/nn404889b
10. Liu, Y., Yu, D., Zeng, C., Miao, Z., & Dai, L. (2010). Biocompatible Graphene Oxide-Based Glucose Biosensors. *Langmuir*, 26(9), 6158-6160. doi:10.1021/la100886x
11. Shan, C., Yang, H., Song, J., Han, D., Ivaska, A., & Niu, L. (2009). Direct Electrochemistry of Glucose Oxidase and Biosensing for Glucose Based on Graphene. *Analytical Chemistry*, 81(6), 2378-2382. doi:10.1021/ac802193c
12. Sun, B., Gou, Y., Ma, Y., Zheng, X., Bai, R., Ahmed Abdelmoaty, A. A., & Hu, F. (2017). Investigate electrochemical immunosensor of cortisol based on gold nanoparticles/magnetic functionalized reduced graphene oxide. *Biosens Bioelectron*, 88, 55-62. doi:10.1016/j.bios.2016.07.047
13. Li, Q., Hong, L., Li, H., & Liu, C. (2017). Graphene oxide-fullerene C60 (GO-C60) hybrid for photodynamic and photothermal therapy triggered by near-infrared light. *Biosens Bioelectron*, 89(Pt 1), 477-482. doi:10.1016/j.bios.2016.03.072
14. Li, M., Yang, X., Ren, J., Qu, K., & Qu, X. (2012). Using Graphene Oxide High Near-Infrared Absorbance for Photothermal Treatment of Alzheimer's Disease. *Advanced Materials*, 24(13), 1722-1728. doi:10.1002/adma.201104864
15. Liu, S., Zeng, T. H., Hofmann, M., Burcombe, E., Wei, J., Jiang, R., . . . Chen, Y. (2011). Antibacterial Activity of Graphite, Graphite Oxide, Graphene Oxide, and Reduced Graphene Oxide: Membrane and Oxidative Stress. *ACS Nano*, 5(9), 6971-6980. doi:10.1021/nn202451x
16. Kim, C., Kim, J. W., Kim, H., Kim, D. H., Choi, C., Jung, Y. S., & Park, J. (2016). Graphene Oxide Assisted Synthesis of Self-assembled Zinc Oxide for Lithium-Ion Battery Anode. *Chemistry of Materials*, 28(23), 8498-8503. doi:10.1021/acs.chemmater.5b03587
17. Lin, Y., Norman, C., Srivastava, D., Azough, F., Wang, L., Robbins, M., . . . Kinloch, I. A. (2015). Thermoelectric Power Generation from Lanthanum Strontium Titanium Oxide at Room Temperature through the Addition of Graphene. *ACS Applied Materials & Interfaces*, 7(29), 15898-15908. doi:10.1021/acsami.5b03522
18. Hummers, W. S., & Offeman, R. E. (1958). Preparation of graphitic oxide. *Journal of the American Chemical Society*, 1339-1339.
19. Ambrosi, A., & Pumera, M. (2016). Electrochemically Exfoliated Graphene and Graphene Oxide for Energy Storage and Electrochemistry Applications. *Chemistry - A European Journal*, 22(1), 153–159. <https://doi.org/10.1002/chem.201503110>
20. Singh, P. K., Singh, U., Bhattacharya, B., & Rhee, H.-W. (2014). Electrochemical synthesis of graphene oxide and its application as counter electrode in dye sensitized solar cell. *Journal of Renewable and Sustainable Energy*, 6(1). <https://doi.org/10.1063/1.4863834>

21. Yu, P., Tian, Z., Lowe, S. E., Song, J., Ma, Z., Wang, X., . . . Zhong, Y. L. (2016). Mechanically-Assisted Electrochemical Production of Graphene Oxide. *Chemistry of Materials*, 28(22), 8429–8438. doi:10.1021/acs.chemmater.6b04415
22. Quaresma, Sílvia, Vânia André, Auguste Fernandes, and M. Teresa Duarte. "Mechanochemistry – A Green Synthetic Methodology Leading to Metallo drugs, Metallopharmaceuticals and Bio-Inspired Metal-Organic Frameworks." *Inorganica Chimica Acta* 455 (2017): 309–18. <https://doi.org/10.1016/j.ica.2016.09.033>.
23. Pilloni, M., Padella, F., Ennas, G., Lai, S., Bellusci, M., Rombi, E., ... Ferino, I. (2015). Liquid-assisted mechanochemical synthesis of an iron carboxylate Metal Organic Framework and its evaluation in diesel fuel desulfurization. *Microporous and Mesoporous Materials*, 213, 14–21. <https://doi.org/10.1016/j.micromeso.2015.04.005>
24. Tireli, Martina, Marina Juribašić Kulcsár, Nikola Cindro, Davor Gracin, Nikola Biliškov, Mladen Borovina, Manda Ćurić, Ivan Halasz, and Krunoslav Užarević. "Mechanochemical Reactions Studied by in Situ Raman Spectroscopy: Base Catalysis in Liquid-Assisted Grinding." *Chemical Communications* 51, no. 38 (2015): 8058–61. <https://doi.org/10.1039/c5cc01915j>.
25. Andini, S., Bolognese, A., Formisano, D., Manfra, M., Montagnaro, F., & Santoro, L. (2012). Mechanochemistry of ibuprofen pharmaceutical. *Chemosphere*, 88(5), 548–553. <https://doi.org/10.1016/j.chemosphere.2012.03.025>
26. Zwiener, C., & Frimmel, F. H. (2003). Short-term tests with a pilot sewage plant and biofilm reactors for the biological degradation of the pharmaceutical compounds clofibric acid, ibuprofen, and diclofenac. *Science of the Total Environment*, 309(1–3), 201–211. [https://doi.org/10.1016/S0048-9697\(03\)00002-0](https://doi.org/10.1016/S0048-9697(03)00002-0)
27. Caviglioli, G., Valeria, P., Brunella, P., Sergio, C., Attilia, A., & Gaetano, B. (2002). Identification of degradation products of Ibuprofen arising from oxidative and thermal treatments. *Journal of Pharmaceutical and Biomedical Analysis*, 30(3), 499–509. [https://doi.org/10.1016/S0731-7085\(02\)00400-4](https://doi.org/10.1016/S0731-7085(02)00400-4)
28. Zhang, W., Li, C., Liang, M., Geng, Y., & Lu, C. (2010). Preparation of carboxylate-functionalized cellulose via solvent-free mechanochemistry and its characterization as a biosorbent for removal of Pb²⁺ from aqueous solution. *Journal of Hazardous Materials*, 181(1–3), 468–473. <https://doi.org/10.1016/j.jhazmat.2010.05.036>
29. Pasha, M. A., & Datta, B. (2014). Mechanochemistry: An efficient method of solvent-free synthesis of 3-amino-2,4-dicarbonitrile-5-methylbiphenyls. *Journal of Saudi Chemical Society*, 18(1), 47–51. <https://doi.org/10.1016/j.jscs.2011.05.012>
30. Gonçalves, A.G., J.J.M. Órfão, J.L. Figueiredo, O.S.G.P. Soares, M.F.R. Pereira, and R.P. Rocha. "Easy Method to Prepare N-Doped Carbon Nanotubes by Ball Milling." *Carbon* 91 (2015): 114–21. <https://doi.org/10.1016/j.carbon.2015.04.050>.
31. Chae, Ari, Bo Ram Choi, Yujin Choi, Seongho Jo, Eun Bi Kang, Hyukjin Lee, Sung Young Park, and Insik In. "Mechanochemical Synthesis of Fluorescent Carbon Dots from Cellulose Powders." *Nanotechnology* 29, no. 16 (2018). <https://doi.org/10.1088/1361-6528/aaad49>.
32. Tucho, W. M., Mauroy, H., Walmsley, J. C., Deledda, S., Holmestad, R., & Hauback, B. C. (2010). The effects of ball milling intensity on morphology of multiwall carbon nanotubes. *Scripta Materialia*, 63(6), 637–640. <https://doi.org/10.1016/j.scriptamat.2010.05.039>
33. Mondal, O., Mitra, S., Pal, M., Datta, A., Dhara, S., & Chakravorty, D. (2015). Reduced graphene oxide synthesis by high energy ball milling. *Materials Chemistry and Physics*, 161, 123–129. <https://doi.org/10.1016/j.matchemphys.2015.05.023>

34. Sharma, S., & Kothiyal, N. C. (2016). Comparative effects of pristine and ball-milled graphene oxide on physico-chemical characteristics of cement mortar nanocomposites. *Construction and Building Materials*, 115, 256–268. <https://doi.org/10.1016/j.conbuildmat.2016.04.019>
35. Ju, Myung Jong, In Yup Jeon, Kimin Lim, Jae Cheon Kim, Hyun Jung Choi, In Taek Choi, Yu Kyung Eom, et al. "Edge-Carboxylated Graphene Nanoplatelets as Oxygen-Rich Metal-Free Cathodes for Organic Dye-Sensitized Solar Cells." *Energy and Environmental Science* 7, no. 3 (2014): 1044–52. <https://doi.org/10.1039/c3ee43732a>.
36. Seo, J.-M., Kim, M.-J., Dai, L., Jung, S.-M., Choi, H.-J., Baek, J.-B., & Jeon, I.-Y. (2012). Large-Scale Production of Edge-Selectively Functionalized Graphene Nanoplatelets via Ball Milling and Their Use as Metal-Free Electrocatalysts for Oxygen Reduction Reaction. *Journal of the American Chemical Society*, 135(4), 1386–1393. <https://doi.org/10.1021/ja3091643>
37. Bharath, G., Rajesh Madhu, Shen Ming Chen, VEDIYAPPAN VEERAMANI, D. Mangalaraj, and N. Ponpandian. "Solvent-Free Mechanochemical Synthesis of Graphene Oxide and Fe₃O₄ Reduced Graphene Oxide Nanocomposites for Sensitive Detection of Nitrite." *Journal of Materials Chemistry A* 3, no. 30 (2015): 15529–39. <https://doi.org/10.1039/c5ta03179f>.
38. Yan, Lu, Mimi Lin, Chao Zeng, Zhi Chen, Shu Zhang, Xinmei Zhao, Aiguo Wu, et al. "Electroactive and Biocompatible Hydroxyl- Functionalized Graphene by Ball Milling." *Journal of Materials Chemistry* 22, no. 17 (2012): 8367–71. <https://doi.org/10.1039/c2jm30961k>.
39. Dash, Pranita, Tapan Dash, Tapan Kumar Rout, Ashok Kumar Sahu, Surendra Kumar Biswal, and Barada Kanta Mishra. "Preparation of Graphene Oxide by Dry Planetary Ball Milling Process from Natural Graphite." *RSC Advances* 6, no. 15 (2016): 12657–68. <https://doi.org/10.1039/c5ra26491j>.
40. Robinson, J. T., Tabakman, S. M., Liang, Y., Wang, H., Casalongue, H. S., Vinh, D., & Dai, H. (2011). Ultrasmall reduced graphene oxide with high near-infrared absorbance for photothermal therapy. *J Am Chem Soc*, 133(17), 6825–6831. doi:10.1021/ja2010175
41. Wu, M.-C., Deokar, A. R., Liao, J.-H., Shih, P.-Y., & Ling, Y.-C. (2013). Graphene-Based Photothermal Agent for Rapid and Effective Killing of Bacteria. *ACS Nano*, 7(2), 1281–1290. doi:10.1021/nn304782d
42. Xing, R.-G., Li, Y.-N., & Zhang, B.-W. (2017). Preparation of chloro-functionalized reduced graphene oxide by silver-catalyzed radical reaction. *Chinese Chemical Letters*, 28(2), 407–411. doi:10.1016/j.ccllet.2016.10.017
43. Jia, Li, Lini Dong, and Liande Zhu. "Stripping Voltammetry at Graphene Oxide: The Negative Effect of Carbonaceous Debris." *Applied Materials Today* 8 (2017): 26–30. <https://doi.org/10.1016/j.apmt.2017.01.001>.
44. Paredes, J I, S Villar Rodil, A Martínez Alonso, and J M D Tascón. "Graphene Oxide Dispersions in Organic Solvents Partners" 121, no. 18 (2008): 1–2. <https://doi.org/10.1021/la801744a>.
45. Compton, O. C., Jain, B., Dikin, D. A., Abouimrane, A., Amine, K., & Nguyen, S. T. (2011). Chemically active reduced graphene oxide with tunable C/O ratios. *ACS Nano*, 5(6), 4380–4391. <https://doi.org/10.1021/nn1030725>
46. Su, H., Ye, Z., & Hmidi, N. (2017). High-performance iron oxide-graphene oxide nanocomposite adsorbents for arsenic removal. *Colloids and Surfaces A: Physicochemical and Engineering Aspects*, 522, 161–172. <https://doi.org/10.1016/j.colsurfa.2017.02.065>
47. Mei, K.-C., Guo, Y., Bai, J., Costa, P. M., Kafa, H., Protti, A., . . . Al-Jamal, K. T. (2015). Organic Solvent-Free, One-Step Engineering of Graphene-Based Magnetic-Responsive Hybrids Using Design of Experiment-Driven Mechanochemistry. *ACS Applied Materials & Interfaces*, 7(26), 14176–14181. doi:10.1021/acsami.5b03577

48. Grimm, Stefan, Manuel Schweiger, Siegfried Eigler, and Jana Zaumseil. "High-Quality Reduced Graphene Oxide by CVD-Assisted Annealing." *Journal of Physical Chemistry C* 120, no. 5 (2016): 3036–41. <https://doi.org/10.1021/acs.jpcc.5b11598>.
49. Kudin, K. N., Ozbas, B., Schniepp, H. C., Prud, R. K., Aksay, I. A., Car, R., ... Car, R. (2008). Raman spectra of graphite oxide and functionalized graphene sheets. *Nano Letters*, 8(1), 36–41. <https://doi.org/10.1021/nl071822y>
50. Sahoo, Satyaprakash, Geetika Khurana, Sujit K. Barik, S. Dussan, D. Barrionuevo, and Ram S. Katiyar. "In Situ Raman Studies of Electrically Reduced Graphene Oxide and Its Field-Emission Properties." *Journal of Physical Chemistry C* 117, no. 10 (2013): 5485–91. <https://doi.org/10.1021/jp400573w>.
51. Song, Y., Cao, L., Yu, J., Zhang, S., Chen, S., & Jiang, Y. (2017). Amino-functionalized graphene oxide blend with monoethanolamine for efficient carbon dioxide capture. *Journal of Alloys and Compounds*, 704, 245–253.
52. Yu, Huitao, Bangwen Zhang, Chaoke Bulin, Ruihong Li, and Ruiguang Xing. "High-Efficient Synthesis of Graphene Oxide Based on Improved Hummers Method." *Scientific Reports* 6, no. July (2016): 1–7. <https://doi.org/10.1038/srep36143>.
53. Marcano, D. C., Kosynkin, D. V., Berlin, J. M., Sinitskii, A., Sun, Z., Slesarev, A., . . . Tour, J. M. (2010). improved Synthesis of Graphene Oxide. *ACSNANO*, 4(8), 4806-4814.
54. Rubio, Noelia, Rui Serra-Maia, Houmam Kafa, Kuo Ching Mei, Khuloud T. Al-Jamal, William Luckhurst, Mire Zloh, et al. "Production of Water-Soluble Few-Layer Graphene Mesosheets by Dry Milling with Hydrophobic Drug." *Langmuir* 30, no. 49 (2014): 14999–8. <https://doi.org/10.1021/la5038475>.
55. Krishnamoorthy, Karthikeyan, Murugan Veerapandian, Kyusik Yun, and S. J. Kim. "The Chemical and Structural Analysis of Graphene Oxide with Different Degrees of Oxidation." *Carbon* 53 (2013): 38–49. <https://doi.org/10.1016/j.carbon.2012.10.013>.
56. Frindy, S., Primo, A., Ennajih, H., el kacem Qaiss, A., Bouhfid, R., Lahcini, M., ... El Kadib, A. (2017). Chitosan-graphene oxide films and CO₂-dried porous aerogel microspheres: Interfacial interplay and stability. *Carbohydrate Polymers*, 167, 297–305. <https://doi.org/10.1016/j.carbpol.2017.03.034>
57. Aunkor, M. T.H., I. M. Mahbulbul, R. Saidur, and H. S.C. Metselaar. "The Green Reduction of Graphene Oxide." *RSC Advances* 6, no. 33 (2016): 27807–25. <https://doi.org/10.1039/c6ra03189g>.
58. Zhao, Xin, Qinghua Zhang, Dajun Chen, and Ping Lu. "Enhanced Mechanical Properties of Graphene-Based Polyvinyl Alcohol Composites." *Macromolecules* 43, no. 5 (2010): 2357–63. <https://doi.org/10.1021/ma902862u>.
59. Cui, Peng, Junghyun Lee, Eunhee Hwang, and Hyoyoung Lee. "One-Pot Reduction of Graphene Oxide at Subzero Temperatures." *Chemical Communications* 47, no. 45 (2011): 12370–72. <https://doi.org/10.1039/c1cc15569e>.
60. Cervený, Silvina, Fabienne Barroso-Bujans, Ángel Alegría, and Juan Colmenero. "Dynamics of Water Intercalated in Graphite Oxide." *Journal of Physical Chemistry C* 114, no. 6 (2010): 2604–12. <https://doi.org/10.1021/jp907979v>.
61. Tourani, S., A. M. Rashidi, A. A. Safekordi, H. R. Aghabozorg, and F. Khorasheh. "Synthesis of Reduced Graphene Oxide-Carbon Nanotubes (RGO-CNT) Composite and Its Use As a Novel Catalyst Support for Hydro-Purification of Crude Terephthalic Acid." *Industrial and Engineering Chemistry Research* 54, no. 31 (2015): 7591–7603. <https://doi.org/10.1021/acs.iecr.5b01574>.

62. Oppenheimer, P. Goldberg, W. Liu, A. Qadir, Y. W. Sun, Y. Xu, D. J. Dunstan, and C. J. Humphreys. "Effect of Humidity on the Interlayer Interaction of Bilayer Graphene." *Physical Review B* 99, no. 4 (2019): 2–7. <https://doi.org/10.1103/physrevb.99.045402>.
63. Zheng, Sunxiang, Qingsong Tu, Jeffrey J. Urban, Shaofan Li, and Baoxia Mi. "Swelling of Graphene Oxide Membranes in Aqueous Solution: Characterization of Interlayer Spacing and Insight into Water Transport Mechanisms." *ACS Nano* 11, no. 6 (2017): 6440–50. <https://doi.org/10.1021/acs.nano.7b02999>.
64. Acik, Muge, Cecilia Mattevi, Cheng Gong, Geunsik Lee, Kyeongjae Cho, Manish Chhowalla, and Yves J Chabal. "The Role of Intercalated Water in Multilayered Graphene Oxide" *ACS Nano*, no. 10 (2010): 5861–68.